Crystal Structure of a Novel Bacterial Cell-Surface Flagellin Binding to a Polysaccharide[†,‡]

Yukie Maruyama,[§] Misato Momma,[§] Bunzo Mikami,[||] Wataru Hashimoto,[§] and Kousaku Murata*[,§]

Division of Food Science and Biotechnology, Graduate School of Agriculture, Kyoto University, Uji, Kyoto 611-0011, Japan, and Division of Applied Life Sciences, Graduate School of Agriculture, Kyoto University, Uji, Kyoto 611-0011, Japan

Received September 13, 2007; Revised Manuscript Received December 3, 2007

ABSTRACT: Bacterial flagellins are generally self-assembled into extracellular flagella for cell motility. However, the flagellin homologue p5 is found on the cell surface of *Sphingomonas* sp. A1 (strain A1) and binds tightly to the alginate polysaccharide. To assimilate alginate, strain A1 forms a mouthlike pit on the cell surface and concentrates the polymer in the pit. p5 is a candidate receptor that recognizes extracellular alginate and controls pit formation. To improve our understanding of the structure and function of p5, we determined the crystal structure of truncated p5 ($p5\Delta N_{53}C_{45}$) at 2.0 Å resolution. This, to our knowledge, is the first structure of flagellin_IN motif-containing flagellin. $p5\Delta N_{53}C_{45}$ consists of two domains: an α-domain rich in α-helices that forms the N- and C-terminal regions and a β-domain rich in β-strands that constitutes the central region. The α-domain is structurally similar to the D1 domain of *Salmonella typhimurium* flagellin, while the β-domain is structurally similar to the finger domain of the bacteriophage T4 baseplate protein that is important for intermolecular interactions between baseplate and a long or short tail fiber. Results from the deletion mutant analysis suggest that residues 20−40 and 353−363 are responsible for alginate binding. Truncated N- and C-terminal regions are thought to constitute α-helices extending from the α-domain. On the basis of the size and surface charge, the cleft in extended α-helices is proposed as an alginate binding site of p5. Structural similarity in the β-domain suggests that the β-domain is involved in the proper localization and/or orientation of p5 on the cell surface.

Sphingomonas sp. A1 (strain A1) isolated from the soil is a nonmotile Gram-negative bacterium that assimilates alginate (*1*). Alginate is a high-molecular weight linear polysaccharide of α-L-guluronate and its C5 epimer β-D-mannuronate and is produced by brown seaweed and certain bacteria (*2*). Although most alginate-degrading microbes such as marine bacteria, soil bacteria, and fungi produce alginate lyase in the extracellular and/or periplasmic fractions, i.e., outside the cytoplasmic membrane (*3*, *4*), strain A1 alginate lyases are exclusively localized in the cytoplasm. Strain A1 differs from other alginate-degrading microbes with respect to the alginate import and degradation pathway. To assimilate alginate, strain A1 forms a mouthlike pit (0.02−0.1 μm) on the cell surface. An external alginate polymer concentrated in the pit is directly incorporated into the cytoplasm through the action of periplasmic alginate-binding proteins and an inner membrane ATP-binding cassette (ABC)[1] transporter (*5*, *6*). The polymer is then degraded into monosaccharides through the action of intracellular exo- and endo-type alginate lyases (*7*, *8*). This alginate import system is peculiar since, generally, microbes assimilate macromolecules by secreting extracellular degrading enzymes and subsequently incorporating their degradation products into the cell. Genes for the proteins involved in alginate uptake and degradation form a single cluster. This gene cluster has also been found in the genome of *Agrobacterium tumefaciens* (*9*), suggesting that the pit observed in strain A1 is latent in several bacteria. Some sphingomonads transformed with a plasmid containing the strain A1 gene cluster formed a pit on their cell surface (*10*). However, pit formation in these transformants is independent of alginate, indicating that alginate-dependent pit formation and disappearance in strain A1 are controlled by factors other than the gene cluster. Such factors include a receptor for alginate. To understand this novel macromolecule import system, it is important to elucidate the mechanism employed by strain A1 for polysaccharide recognition and regulation of pit formation.

Recently, to clarify the details of the overall alginate import system in strain A1, we performed a proteomics-based analysis that focused on strain A1 outer membrane proteins (*11*). This led to the identification of eight cell-surface

[†]This work was supported in part by Research Fellowships from the Japan Society for the Promotion of Science for Young Scientists (Y.M.) and by Grants-in-Aid (K.M. and B.M.) and the Targeted Proteins Research Program (W.H.) from the Ministry of Education, Culture, Sports, Science, and Technology of Japan. X-ray diffraction data were collected at beamline BL38B1 of SPring-8 under the approval of *JASRI* (Proposals 2006A1150 and 2006B1126).

[‡]The atomic coordinates and observed structure factors of $p5\Delta N_{53}C_{45}$ have been deposited in the RCSB Protein Data Bank as entry 2ZBI.

* To whom correspondence should be addressed. E-Mail: kmurata@kais.kyoto-u.ac.jp. Fax: +81-774-38-3767. Phone: +81-774-38-3766.

[§] Division of Food Science and Biotechnology.

[||] Division of Applied Life Sciences.

[1] Abbreviations: ABC, ATP-binding cassette; PCR, polymerase chain reaction; Tris, tris(hydroxymethyl)aminomethane; SDS−PAGE, sodium dodecyl sulfate−polyacrylamide gel electrophoresis; MES, 2-morpholinoethanesulfonic acid; CD, circular dichroism; SPR, surface plasmon resonance; RU, resonance unit; HAP, hook-associated protein; SeMet, selenomethionine; rmsd, root-mean-square deviation.

10.1021/bi701872x CCC: $40.75
Published on Web 01/12/2008

Table 1: Plasmid and Primers Used for Construction of the Expression Plasmid and Absorption Coefficients of Purified Mutant Proteins

protein	template plasmid	forward primer	reverse primer	resultant plasmid	absorption coefficient (1 mg/mL)[b]
$p5\Delta N_{53}$	pET21b-p5[a]	5′-ATGACCGCTCAGATCAAGGCTCTGA-3′	5′-ATGTATATCTCCTTCTTAAAGTTAA-3′	pET21b-$p5\Delta N_{53}$	0.248
$p5\Delta C_{45}$	pET21b-p5[a]	5′-CTCGAGCACCACCACCACCACTGAGAT-3′	5′-ACGTGCGGACGACAGGTTCTCGGTC-3′	pET21b-$p5\Delta C_{45}$	0.241
$p5\Delta N_{53}C_{45}$	pET21b-$p5\Delta N_{53}$	5′-CTCGAGCACCACCACCACCACTGAGAT-3′	5′-ACGTGCGGACGACAGGTTCTCGGTC-3′	pET21b-$p5\Delta N_{53}C_{45}$	0.287
$p5\Delta N_{53}C_{10}$	pET21b-$p5\Delta N_{53}$	5′-ATGACCGCTCAGATCAAGGCTCTGA-3′	5′-CGCGTTGGCTTGAGCCAGCATCGC-3′	pET21b-$p5\Delta N_{53}C_{10}$	0.257
$p5\Delta N_{53}C_{20}$	pET21b-$p5\Delta N_{53}$	5′-ATGACCGCTCAGATCAAGGCTCTGA-3′	5′-GGCCTGTTGCAGAATCTGAGCGCG-3′	pET21b-$p5\Delta N_{53}C_{20}$	0.264
$p5\Delta N_{53}C_{30}$	pET21b-$p5\Delta N_{53}$	5′-ATGACCGCTCAGATCAAGGCTCTGA-3′	5′-GTTAGCGGTTTCCGAGGCGAAGTC-3′	pET21b-$p5\Delta N_{53}C_{30}$	0.274
$p5\Delta N_{10}C_{45}$	pET21b-$p5\Delta C_{45}$	5′-TCCCTGAACGCGCAACGCAACATC-3′	5′-CATATGTATATCTCCTTCTTAAAGTTAA-3′	pET21b-$p5\Delta N_{10}C_{45}$	0.250
$p5\Delta N_{20}C_{45}$	pET21b-$p5\Delta C_{45}$	5′-ACGCAGAACTCGCTGTCGACGTCG-3′	5′-CATATGTATATCTCCTTCTTAAAGTTAA-3′	pET21b-$p5\Delta N_{20}C_{45}$	0.258
$p5\Delta N_{30}C_{45}$	pET21b-$p5\Delta C_{45}$	5′-CGCTTGTCCTCCGGCCTGCGCATC-3′	5′-CATATGTATATCTCCTTCTTAAAGTTAA-3′	pET21b-$p5\Delta N_{30}C_{45}$	0.267
$p5\Delta N_{40}C_{45}$	pET21b-$p5\Delta C_{45}$	5′-GCCAAGGACGACGCTGCCGGCCTG-3′	5′-CATATGTATATCTCCTTCTTAAAGTTAA-3′	pET21b-$p5\Delta N_{40}C_{45}$	0.277

[a] pET21b plasmid containing the p5 coding region. [b] These values were calculated using ProtParam (http://kr.expasy.org/tools/protparam.html).

proteins whose expression was found to be alginate-dependent (*11*, *12*). Unexpectedly, two of these proteins turned out to be homologues of a bacterial flagellar protein, i.e., flagellin, although strain A1 cells grown in different media show no motility or flagellum formation. As in the case of human receptor CD44 that binds to the acidic polysaccharide hyaluronan (*13*), strain A1 flagellin homologues, which were designated p5 and p6, were experimentally confirmed to have high-affinity interactions with alginate ($K_d \sim 10^{-9}$ M) (*11*). Immunoelectron microscopy using an anti-p5 antibody indicated that strain A1 flagellin homologues are exclusively localized on the cell surface. These findings suggest that p5 and p6 recognize external alginate as receptors on the cell surface and are distinct from bacterial flagellins that constitute helical flagellar filaments (*11*).

The bacterial flagellum is an extracellular organelle that facilitates motility. In addition to cell motility, flagella are known to be involved in other biological functions of bacteria such as host adhesion, colonization, and virulence (*14*). The bacterial flagellar filament is a tubular structure composed of several thousand flagellin subunits (*15*). Filament assembly is involved in the passage of the newly generated flagellin through a central channel. Although many extensive structural studies on bacterial flagellin have been performed, only one three-dimensional structure of *Salmonella typhimurium* flagellin has been determined by X-ray crystallography and electron cryomicroscopy (*16*, *17*). Bacterial flagellin consists of four structural domains, i.e., D0, D1, D2, and D3. The N-terminal chain starts from D0, passes through D1 and D2, and reaches D3. It then returns through D2 and D1, and the C-terminal chain ends in D0 (*17*). The D0 and D1 domains are crucial for self-assembly. The N- and C-terminal regions, which contain ~50 residues each, constitute the D0 domain and are rich in hydrophobic residues and thus interact hydrophobically with other flagellin subunits in the filament (*16*, *17*). D0 domain-truncated flagellins fail to form a stable filament (*18*). Due to restrictions on filament formation and molecular passage inside the filaments, amino acid sequences in the D0 and D1 domains are highly conserved among diverse bacteria, whereas the solvent-exposed central D2 and D3 domains vary in sequence and length. This is also true of strain A1 flagellin homologues p5 and p6; however, these homologues differ from bacterial flagellated flagellins in terms of function and localization.

Analysis of the structure−function relationship of strain A1 flagellin homologues would contribute to elucidation of the mechanisms of alginate recognition and pit formation and also to understanding of the diversity of bacterial flagellins in terms of structure and function. In this study, to obtain information about the structural factors of strain A1 flagellin homologues involved in alginate binding and cell-surface localization, we carried out a deletion mutant analysis and X-ray crystallographic studies on p5. As a result, we determined the crystal structure of the N- and C-terminal truncated mutant p5 ($p5\Delta N_{53}C_{45}$). Although $p5\Delta N_{53}C_{45}$ lacks the alginate-binding domain identified by deletion mutant analysis, a homology model for the missing parts of p5 suggests that the cleft in extended α-helices is an alginate binding site. We also discuss the role of the central domain of p5 on the basis of its structural homology with the T4 phage protein.

EXPERIMENTAL PROCEDURES

Construction, Expression, and Purification of Deletion Mutants of p5. Mutants of p5 were constructed by the polymerase chain reaction (PCR). The plasmid and primers used for the amplification of individual genes are summarized in Table 1. A linear fragment amplified by PCR using each primer set and KOD plus DNA polymerase (Toyobo, Tokyo, Japan) contained the truncated p5 gene inserted in pET21b. The PCR was performed according to the manufacturer's instructions for KOD plus DNA polymerase, and the conditions were as follows: 30 cycles of denaturation (94 °C for 15 s), annealing (55 °C for 30 s), and elongation (68 °C for 6 min). The DNA fragment was self-ligated after treatment with the T4 DNA polynucleotide kinase (Toyobo). *Escherichia coli* BL21(DE3) cells were transformed with each plasmid. For structure determination, the selenomethionine (SeMet)-labeled p5$\Delta N_{53}C_{45}$ was prepared by transforming the methionine-requiring auxotroph *E. coli* B384(DE3) with pET21b-p5$\Delta N_{53}C_{45}$. The nucleotide sequences of p5 mutant genes were determined by dideoxy chain termination using an automated DNA sequencer (model 377, Applied Biosystems, Foster City, CA) (*19*). Subcloning, transformation, and gel electrophoresis were carried out as described elsewhere (*20*). Since the pET21b vector was designed to express a fusion protein with a histidine-tagged sequence at the C-terminus, *E. coli* transformants thus constructed produced p5 with a histidine-tagged sequence at the C-terminus.

E. coli cells transformed with the wild-type or mutant p5 gene were cultivated and harvested as described elsewhere (*11*). LB medium was used for BL21(DE3) cultivation, and minimal medium containing SeMet (25 mg/L) was used for B384(DE3) (*21*). The harvested cells were suspended in 20 mM Tris-HCl (pH 8.0) and ultrasonically disrupted (model 201M insonator, Kubota, Kyoto, Japan) at 0 °C and 9 kHz for 20 min. The cell extracts were applied to a DEAE-Toyopearl 650M column (Tosoh Co., Tokyo, Japan) equilibrated with 20 mM Tris-HCl (pH 8.0). The protein was eluted with a linear gradient of NaCl (0 to 0.5 M) in 20 mM Tris-HCl (pH 8.0) at 4 °C. Fractions containing p5 or one of its mutants were identified by sodium dodecyl sulfate−polyacrylamide gel electrophoresis (SDS−PAGE) followed by staining with Coomassie brilliant blue. After the fractions containing significant amounts of p5 or one of its mutants had been pooled, a 500 mM imidazole solution was added to the protein solution to give a final concentration of 50 mM. The protein solution was then applied to a column of Ni^{2+} ion-bound chelating Sepharose Fast Flow (GE Healthcare, Buckinghamshire, England) that had been pre-equilibrated with 20 mM Tris-HCl (pH 8.0) containing 500 mM NaCl and 50 mM imidazole. The protein was eluted with a linear gradient of imidazole (50 to 500 mM) in 20 mM Tris-HCl (pH 8.0) containing 500 mM NaCl. The protein fractions were analyzed by SDS−PAGE and pooled. The protein was further purified using a Mono Q 10/100 column (GE Healthcare) that had been pre-equilibrated with 20 mM Tris-HCl (pH 8.0). The protein was eluted with a linear gradient of NaCl (0 to 0.7 M) in the same buffer. Fractions containing purified p5 or one of its mutants were pooled and dialyzed against 20 mM Tris-HCl (pH 8.0).

Measurement of Protein Concentration. Protein concentration was determined by measuring the absorbance at 280 nm. The absorption coefficient for 1 mg/mL p5 was determined to be 0.208 by ProtParam (http://kr.expasy.org/tools/protparam.html), and the values for all the p5 mutants are listed in Table 1.

Self-Assembly Analysis. To analyze the self-assembly of wild-type p5 and its mutants, we subjected the purified proteins to gel filtration column chromatography on a Superdex 200 10/300 column (GE Healthcare) that had been pre-equilibrated with 10 mM 2-morpholinoethanesulfonic acid-NaOH (MES-NaOH) (pH 6.0) containing 0.15 M NaCl at a flow rate of 0.5 mL/min. Proteins were dialyzed against 10 mM MES-NaOH (pH 6.0) at 4 °C prior to gel filtration column chromatography.

Circular Dichroism (CD) Spectropolarimetry. The secondary structures of wild-type p5 and its mutants were evaluated by CD spectroscopy. CD spectra were recorded with a Jasco (Tokyo, Japan) model J720 spectropolarimeter. The far-UV spectra were recorded between 190 and 260 nm using a demountable quartz cell with a path length of 0.1 mm. The protein concentration was adjusted to 1.0 mg/mL in 10 mM MES-NaOH (pH 6.0) containing 0.15 M NaCl.

Surface Plasmon Resonance (SPR) Biosensor Analysis. The SPR biosensor analysis was conducted at 25 °C using CM5 sensor chips on a Biacore 2000 instrument (Biacore International AB, Uppsala, Sweden). Each purified protein was immobilized on a sensor chip by standard amine coupling as follows. The dextran surface was activated by adding 50 μL of a mixture of 0.05 M *N*-hydroxysuccinimide and 0.2 M ethyl 3-[3-(dimethylamino)propyl]carbodiimide. The purified protein (50 μg/mL, 100 μL) in 10 mM sodium acetate (pH 5.0) was injected, followed by the addition of ethanolamine (50 μL) to block any remaining activated groups on the dextran surface. The HBS-EP buffer [10 mM HEPES (pH 7.4), 150 mM NaCl, 3 mM EDTA, and 0.005% surfactant p20] was used as the running buffer for immobilization at a flow rate of 5 μL/min. Each protein was immobilized in the dextran matrix on the sensor chip at 3000 resonance units (RU) for wild-type p5, 1890 for p5ΔN_{53}, 1680 for p5$\Delta N_{53}C_{20}$, 740 for p5$\Delta N_{53}C_{30}$, 5020 for p5ΔC_{45}, 3780 for p5$\Delta N_{10}C_{45}$, 1680 for p5$\Delta N_{20}C_{45}$, 610 for p5$\Delta N_{40}C_{45}$, and 1800 for p5$\Delta N_{53}C_{43}$. The protein−alginate interaction was assessed using 10 mM MES-NaOH (pH 6.0) or sodium acetate (pH 4.0) containing 150 mM NaCl and 0.005% Tween 20 as the running buffer at a flow rate of 20 μL/min. Alginate (Nacalai, Kyoto, Japan) dissolved in the running buffer was injected for 2 min, and the dissociation was monitored for 5 min. After each binding assay cycle, the sensor chip surface was regenerated by adding 30 μL of 100 mM Tris-HCl (pH 8.0) at a flow rate of 20 μL/min. All binding data were subtracted from the level of binding to a blank flow cell.

X-ray Crystallography. SeMet-substituted p5$\Delta N_{53}C_{45}$ was crystallized by hanging-drop vapor diffusion. Single crystals were obtained at 20 °C in a mixture of protein solution (3 μL) and mother liquor (3 μL) [28% polyethylene glycol 5000 monomethyl ether, 0.2 M ammonium sulfate, and 0.1 M MES-NaOH (pH 6.5)]. The initial protein concentration was 18 mg/mL. The crystal was flash-frozen under a cold nitrogen stream and stored in liquid nitrogen. Diffraction data were collected at a λ of 0.97906 Å using a Jupiter 210 CCD

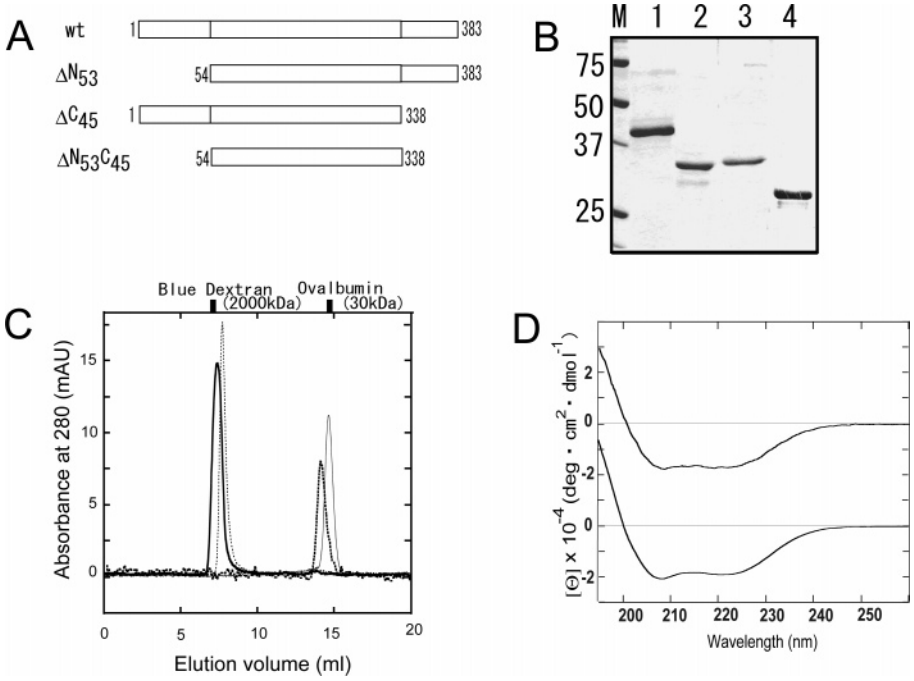

FIGURE 1: Construction and structural characterization of p5 mutants. (A) Schematic design of deletions. (B) SDS−PAGE of purified wild-type p5 and its mutants: lane M, molecular markers; lane 1, wild-type p5; lane 2, p5ΔN_{53}; lane 3, p5ΔC_{45}; and lane 4, p5$\Delta N_{53}C_{45}$. Numbers on the left indicate the molecular mass (kilodaltons). (C) Gel filtration patterns of wild-type p5 and its mutants: thick solid line, wild-type p5; thick dashed line, p5ΔN_{53}; thin dashed line, p5ΔC_{45}; and thin solid line, p5$\Delta N_{53}C_{45}$. (D) Far-UV CD spectra of wild-type p5 (top trace) and p5$\Delta N_{53}C_{45}$ (bottom trace).

detector at the BL38B1 station of SPring-8 (Harima, Japan). Diffraction data were indexed, integrated, and scaled with HKL2000 (*22*). The space group of the crystal was determined to be *P*1 with the following unit cell dimensions: $a = 32.49$ Å, $b = 52.17$ Å, $c = 76.20$ Å, $\alpha = 99.11°$, $\beta = 93.90°$, and $\gamma = 107.97°$. There were two p5$\Delta N_{53}C_{45}$ monomers per crystallographic asymmetric unit. The SHELXD program (*23*) showed that there were two Se atoms per monomer. Phases were computed to 2.0 Å resolution with SHELXE (*24*). Subsequent solvent flattening was conducted with DM (*25*). Models of ordered residues were built manually using winCoot (*26*). The model was refined with REFMAC5 (*27*). A randomly selected 5% of the reflections were excluded from refinement and used to calculate R_{free}. After several rounds of energy minimization and manual model building, isolated electron densities exceeding 3σ on the $F_o - F_c$ map and/or 1.2σ on the $2F_o - F_c$ map were assigned as water molecules when their locations were sterically reasonable. The final model quality was checked using PROCHECK (*28*). Figures for protein structures were prepared using PyMol (*29*).

RESULTS

Structural Assignment of p5 Mutants. Previously, we found that the flagellin homologues p5 and p6 were expressed on the cell surface of strain A1 (*11*). Both proteins exhibit a high affinity for alginate. In addition to p5 and p6, *E. coli* flagellin also binds to alginate with a binding affinity in the nanomolar range, suggesting that bacterial flagellins share common characteristics with respect to the binding of polysaccharides. Since the amino acid sequences of the N- and C-terminal regions are highly conserved in many bacterial flagellins, it is possible that these regions play an important role in polysaccharide binding. To determine the effects of conserved N- and/or C-terminal regions on alginate affinity, we constructed three deletion mutants that lacked one or both regions (Figure 1A). Recombinant mutant proteins were expressed in *E. coli* cells and purified using anion exchange and affinity chromatography (Figure 1B).

In addition to in vivo polymerization, *Salmonella* flagellin is known to polymerize into a flagellar filament in vitro (*30*), but its deletion mutant that lacked the N- and C-terminal regions was unable to form a filament (*18*). We therefore checked the self-assembly of p5 by using gel filtration column chromatography (Figure 1C). We found that purified wild-type p5 and p5ΔC_{45} were eluted in the void volume, indicating their polymerization. However, p5ΔN_{53} and p5$\Delta N_{53}C_{45}$ were found to be monomeric.

To confirm that the folding was correct, we measured the far-UV CD spectra of the mutants (Figure 1D). The CD spectra of all mutants were essentially equivalent, indicating that the deletions had no effect on the secondary structure of p5. The spectra showed minima at 208 and 222 nm, the heights of which were almost equal, suggesting the abundance of α-helices in p5.

Overall Structure of p5$\Delta N_{53}C_{45}$. To determine the three-dimensional structure, initial crystallization screenings were carried out for wild-type p5 and all its mutants. Among these, p5$\Delta N_{53}C_{45}$ formed single crystals that were suitable for structure determination. Because we failed to determine the structure by molecular replacement using the crystal structure of *Salmonella* flagellin, we determined the crystal structure of SeMet-substituted p5$\Delta N_{53}C_{45}$ by using the single-wavelength anomalous diffraction method at 2.0 Å resolution. The statistics for data collection and structure refinement are summarized in Table 2. Each asymmetric unit has two monomers. The final model contains 530 amino acid residues (265 per monomer) and 344 water molecules. No electron

Table 2: Overview of Data Collection and Refinement Statistics[a]

Data Collection	
wavelength (Å)	0.97906
space group	*P*1
unit cell dimensions	$a = 32.49$ Å, $b = 52.17$ Å, $c = 76.20$ Å, $\alpha = 99.11°$, $\beta = 93.90°$, $\gamma = 107.97°$
no. of observed reflections	113599
no. of unique reflections	61347
resolution (Å)	50.0−2.0 (2.07−2.00)
R_{sym}	0.051 (0.19)
completeness (%)	97.4 (93.5)
I/σ	23.9
Wilson *B* factor (Å^2)	17.1
Refinement Statistics	
R_{cryst}	0.197 (0.25)
R_{free}	0.283 (0.31)
rmsd for bond lengths (Å)	0.018
rmsd for bond angles (deg)	1.743
average *B* (Å^2)/no. of atoms	
proteins	15.8/3855
water molecules	21.2/344
Ramachandran plot (%)	
most favored regions	91.3
additional allowed regions	8.3
generously allowed regions	0.4

[a] Values for the outer resolution shell are given in parentheses.

density was observed for eight N-terminal and 12 C-terminal residues. N-Terminal sequencing and Western blotting using an antibody for the C-terminal His tag showed that these residues were present but were flexible in the crystal.

The ribbon diagrams of the overall structure and topology of the secondary structure elements of $p5\Delta N_{53}C_{45}$ are shown in panels A and B of Figure 2. The protein has dimensions of approximately 30 Å × 30 Å × 82 Å. The $p5\Delta N_{53}C_{45}$ protein is divided into two structural domains connected by two short peptide linkers. The terminal domain (α-domain) consists of residues 62−167 and residues 283−326. The N-terminal part of the α-domain forms two long α-helices (H1 and H2) that are arranged in an antiparallel fashion and are followed by two β-hairpins (S1 and S2, and S3 and S4), and the C-terminal part forms an α-helix (H5), which greatly resembles the D1 domain of *Salmonella* flagellin (Figure 2C) (*16*). On the other hand, the central domain (β-domain, residues 173−281) between the N- and C-terminal parts of the α-domain significantly differs from the D2 and D3 domains of *Salmonella* flagellin, although each consists mainly of β-strands. The β-domain contains two antiparallel β-sheets, i.e., sheets A and B (Figure 2B), which sandwich an α-helix (H3). Each β-sheet consists of four strands (SA1−SA4 and SB1−SB4). A longer helix (H3) is present between the two β-sheets, and a shorter helix (H4) connects two strands (SB2 and SB1) of sheet B.

Construction of the Entire p5 Model. When $p5\Delta N_{53}C_{45}$ and *Salmonella* flagellin (PDB entry 1UCU) were superimposed using the Cα atoms of the α-domain of $p5\Delta N_{53}C_{45}$ and the D1 domain of the flagellin, the root-mean-square deviation (rmsd) was 1.45 Å for 125 Cα atoms, indicating that the backbone structures for these domains are essentially the same; this is consistent with the observation that the amino acid sequences of these domains are highly conserved. The primary structures of the D0 domain are also highly conserved among the flagellins, including p5. This strongly suggests that the truncated N- and C-terminal regions in $p5\Delta N_{53}C_{45}$ fold into α-helices in wild-type p5 in the same way as the D0 domain of *Salmonella* flagellin. We thus referenced the model of the superimposed *Salmonella* flagellin and constructed a model of the p5 N- and C-terminal regions with its amino acid sequence (Figure 2D). The entire p5 model is thought to be long and thin (approximately 30 Å × 30 Å × 160 Å), similar to a matchstick.

Structural Comparison of the β-Domain. To structurally characterize the β-domain, we searched the homologous structure of the β-domain of $p5\Delta N_{53}C_{45}$ using the DALI program (http://www.ebi.ac.uk/dali/). Significant similarity was detected only in the structure of the finger domain of gp11, which is a baseplate protein of bacteriophage T4 (Figure 3A,B) (*31*), with a *Z* value of 4.6 and a reference amino acid length of 90. As shown in Figures 2B and 3B, the topologies of the p5 β-domain and the gp11 finger domain are similar, although their latter half is somewhat different. Most similar parts of these domains, i.e., SA2, SB3, SB4, H3, SA4, and SA3 (residues 173−249) in the p5 β-domain and β3, β5, β4, α4, β6, and β7 (residues 81−160) in the gp11 finger domain, superimpose well (Figure 3C), and the rmsd between them is 2.7 Å for 57 corresponding Cα atoms. However, the primary structures of the β-domain of p5 and the finger domain of gp11 show little similarity even in the region where the three-dimensional structures are most similar (Figure 3D). The gp11 protein binds to a short tail fiber protein (gp12) and another baseplate structural protein (gp10) to connect both proteins when the T4 phage is in solution. When the T4 phage attaches to the host cell surface, gp11 dissociates from the short tail fiber protein (gp12) and binds to a long tail fiber protein (gp34) to connect the baseplate and long tail fiber. In a series of conformational transitions that occur upon adsorption of the T4 phage onto the host cell surface, the finger domain of gp11 is thought to invariably bind to gp10 (*32*−*34*).

Alginate Binding. The p5 protein binds to alginate under acidic conditions at pH <6.0 with a peak at pH 4.0 (*11*). Considering the nonspecific electrostatic interactions between proteins and the acidic polysaccharide (alginate), we measured the alginate binding ability of p5 deletion mutants by SPR analysis using MES-NaOH buffer containing 0.15 M NaCl and 0.005% Tween 20 at pH 6.0, a pH that is significantly higher than the p*I* of p5 (4.75). Alginate was bound to $p5\Delta N_{53}$ and $p5\Delta C_{45}$ as well as to wild-type p5 (Figure 4A) but not to $p5\Delta N_{53}C_{45}$. No interaction was observed between $p5\Delta N_{53}C_{45}$ and alginate even at pH 4.0.

To investigate the binding site of alginate on p5, we constructed seven additional mutants in *E. coli* cells (Figure 4B). The protein that was expressed was checked using the anti-His tag antibody. Of these mutants, little $p5\Delta N_{30}C_{45}$ and $p5\Delta N_{53}C_{10}$ expression was observed in *E. coli*. The other five mutants were purified by anion exchange and affinity chromatography (Figure 4C). Gel filtration column chromatography showed all five mutants to be present as monomers, and by measuring the far-UV CD spectra, we confirmed that their secondary structures were comparable to those of wild-type p5. The $p5\Delta N_{10}C_{45}$, $p5\Delta N_{20}C_{45}$, and $p5\Delta N_{53}C_{20}$ mutants interacted with alginate at pH 6.0, although $p5\Delta N_{40}C_{45}$ and $p5\Delta N_{53}C_{30}$ did not (Figure 4D). This observation indicates that residues 20−40 and 353−363 of p5 are important for alginate binding. The lack of alginate binding by $p5\Delta N_{40}C_{45}$, $p5\Delta N_{53}C_{30}$, and $p5\Delta N_{53}C_{45}$ is not due to structural disorder

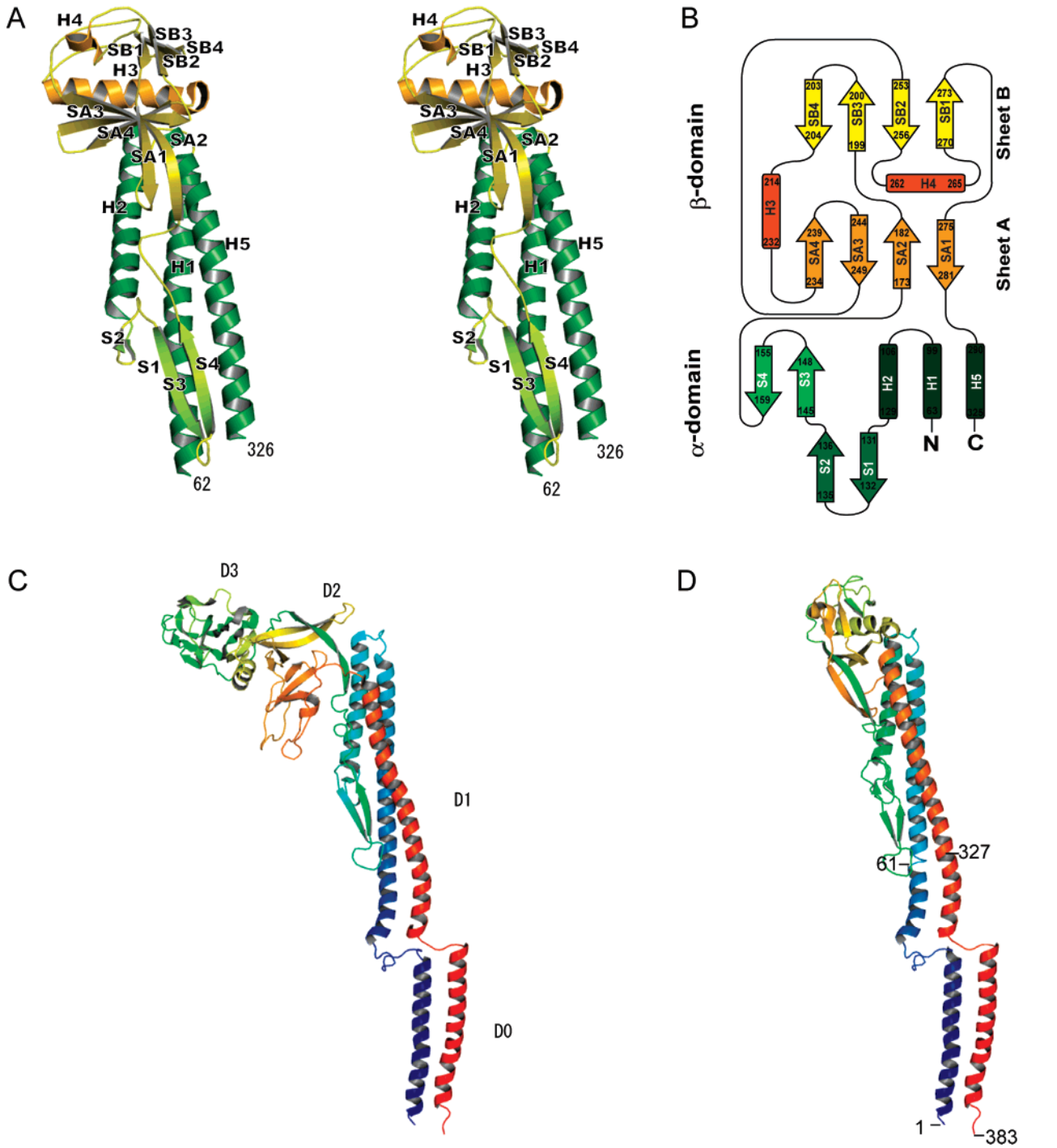

FIGURE 2: Overall structure of p5 and *Salmonella* flagellin. (A) Ribbon diagram (wall-eye stereoview) of $p5\Delta N_{53}C_{45}$. The terminal α-domain is colored green, and the central *β*-domain is colored yellow. The model starts from Thr62 and ends at Ala326. (B) Topology of the secondary structure of $p5\Delta N_{53}C_{45}$. (C) Ribbon diagram of *Salmonella* flagellin (PDB entry 1UCU) with the domain nomenclature. (D) Homology model of wild-type p5. Residues 1−61 and 327−383 are modeled on the basis of the coordinates of *Salmonella* flagellin. The chain in panels C and D is color-coded from blue to red from the N-terminus to the C-terminus. Both structures in panels C and D are shown on the same scale and in the same orientation.

caused by the long deletion because no significant difference was observed between the secondary structures of mutants and wild-type p5. Similarly, p5 polymerization is not essential for alginate recognition because no correlation exists between self-assembly and alginate binding.

DISCUSSION

Flagellin_IN Motif Structure. Three major pfam motifs (http://pfam.cgb.ki.se/), flagellin_N, flagellin_IN, and flagellin_C, are well-known in bacterial flagellins. Almost all flagellins contain the flagellin_N and flagellin_C motifs, while the presence of the flagellin_IN motif varies due to diversity in the central domain. Although this motif varies in sequence, an Ile-Asn pair is present at the center. Some flagellar proteins such as the hook-associated protein (HAP) and flagellin contain several (one to five) flagellin_IN motifs in their molecules. The *β*-domain of p5 contains one flagellin_IN motif that consists of 53 residues. Residues in

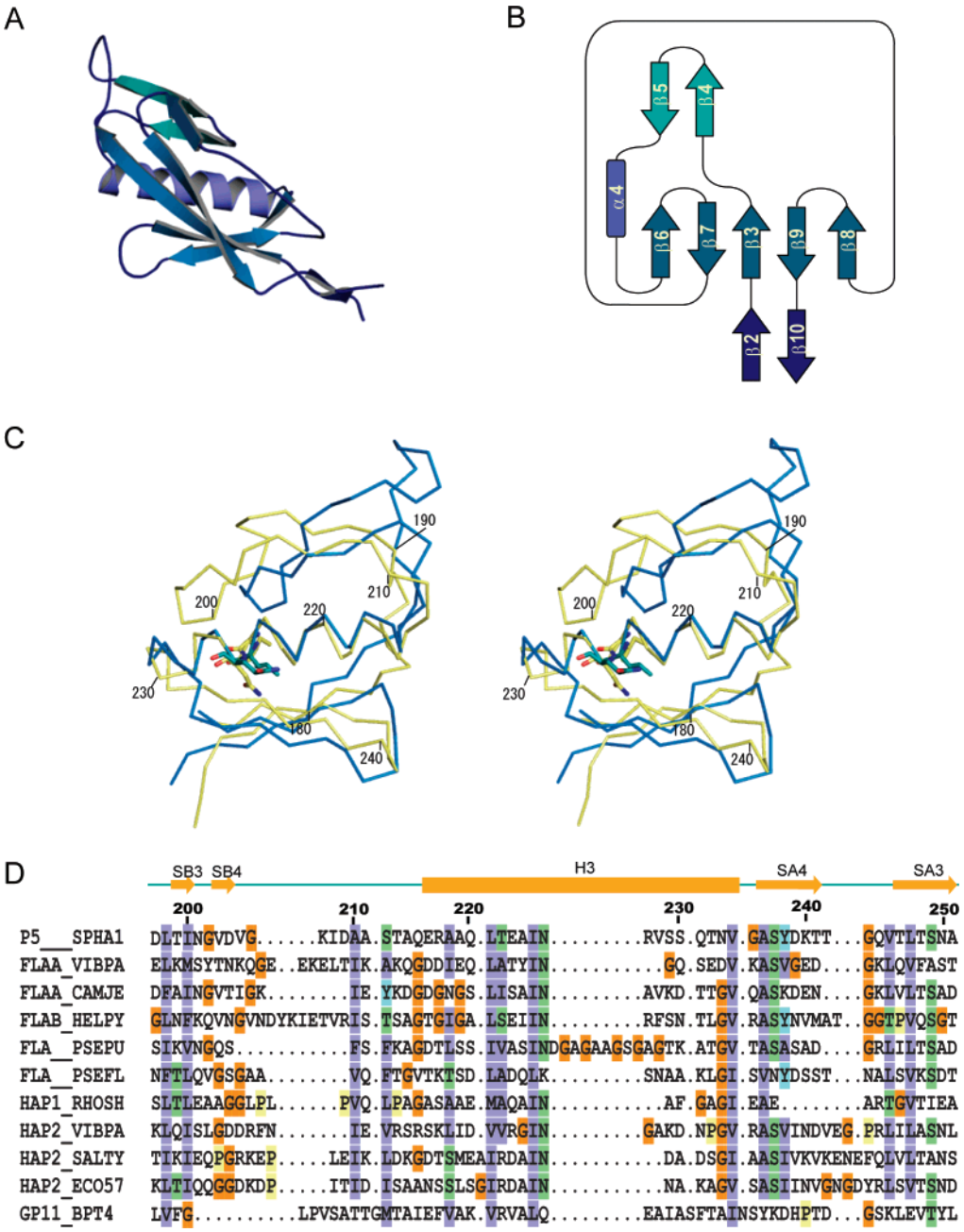

FIGURE 3: Structural comparison of the p5 β-domain and gp11 finger domain. (A) Three-dimensional structure of the gp11 finger domain (PDB entry 1EL6). (B) Topology of the secondary structure of the gp11 finger domain. (C) Wall-eye stereoview of the superimposition of the β-domain (yellow) and the finger domain (blue). Residues 173−249 of p5 and 81−160 of gp11 are represented in the figure. An Ile-Asn pair at the center of the Flagellin_IN motif of p5, and the corresponding amino acid residues of gp11 are shown as a stick model (p5, yellow; gp11, blue). (D) Sequence alignment of the flagellin_IN motif and the corresponding residues in gp11: P5_SPHA1, p5; FLAA_VIBPA, flagellin A from *Vibrio parahaemolyticus*; FLAA_CAMJE, flagellin A from *Campylobacter jejuni*; FLAB_HELPY, flagellin B from *Helicobacter pylori*; FLA_PSEFL, flagellin from *Pseudomonas fluorescens*; HAP1_RHOSH, HAP1 from *Rhodobacter sphaeroides*; HAP2_VIBPA, polar flagellar HAP2 from *V. parahaemolyticus*; HAP2_SALTY, HAP2 from *S. typhimurium*; HAP2_ECO57, HAP2 from *E. coli* O157:H7; and GP11_BPT4, gp11 from bacteriophage T4. Residue numbers and the secondary structure assignment of p5 are as indicated. Sequence alignment for p5 and gp11 is based on the three-dimensional structure.

the motif form into strands (SB3 and SB4), a helix (H3), and strands (SA4 and SA3) in $p5\Delta N_{53}C_{45}$, which correspond to residues 197−249. To the best of our knowledge, this is the first determination of the three-dimensional structure of bacterial flagellin with the flagellin_IN motif because *Salmonella* flagellin contains no flagellin_IN motif. The secondary structure elements of β5, α4, and β6 in gp11 correspond to the flagellin_IN motif, but gp11 does not contain the motif (Figure 3D). The fact that the flagellin_IN motif is abundant in flagellar proteins but is absent in structurally similar gp11 suggests that this motif is not necessary for the folding of these proteins. Although the function of the flagellin_IN motif is unknown, the results obtained here may indicate that some biological functions specific to flagella rather than to structure formation restrict amino acid substitution and conserve the motif sequence.

Alginate-Binding Site. As shown by the SPR analysis of deletion mutants, residues 20−40 and 353−363 are crucial for alginate binding. Several basic residues, such as arginine and lysine, are present on the surface around these regions

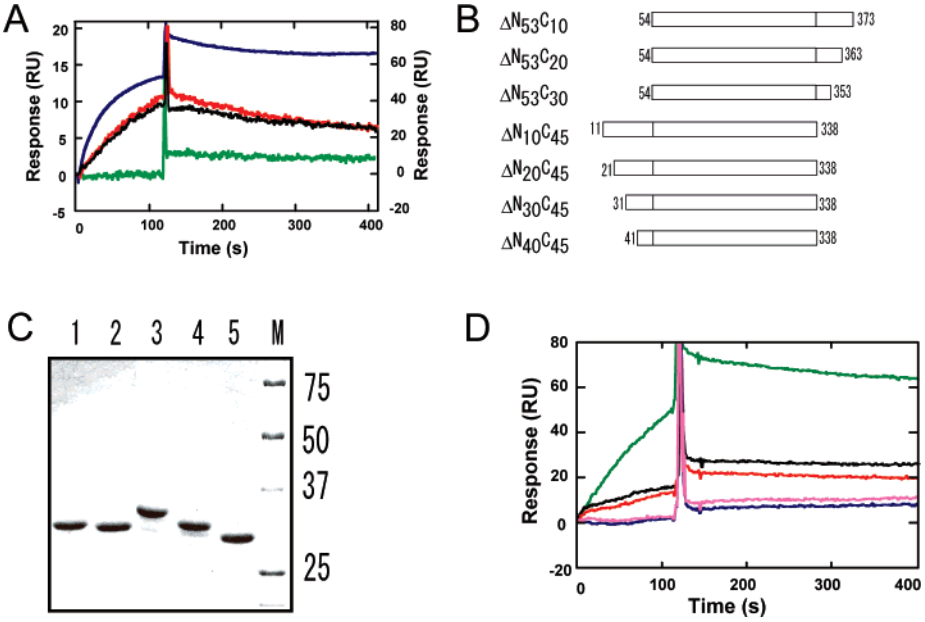

FIGURE 4: Alginate binding ability of p5 and its mutants. (A) SPR analyses of wild-type p5 (black), p5ΔN_{53} (red), p5ΔC_{45} (blue), and p5$\Delta N_{53}C_{45}$ (green). Values on the left indicate the response of wild-type p5, p5ΔN_{53}, and p5$\Delta N_{53}C_{45}$, and those on the right represent that of p5ΔC_{45}. (B) Schematic design of deletion mutants containing different lengths of terminal amino acids. (C) SDS−PAGE of purified mutants: lane M, molecular markers; lane 1, p5$\Delta N_{53}C_{20}$; lane 2, p5$\Delta N_{53}C_{30}$; lane 3, p5$\Delta N_{10}C_{45}$; lane 4, p5$\Delta N_{20}C_{45}$; and lane 5, p5$\Delta N_{40}C_{45}$. Numbers on the right indicate the molecular mass (kilodaltons). (D) SPR analyses of p5$\Delta N_{53}C_{20}$ (red), p5$\Delta N_{53}C_{30}$ (blue), p5$\Delta N_{10}C_{45}$ (green), p5$\Delta N_{20}C_{45}$ (black), and p5$\Delta N_{40}C_{45}$ (pink).

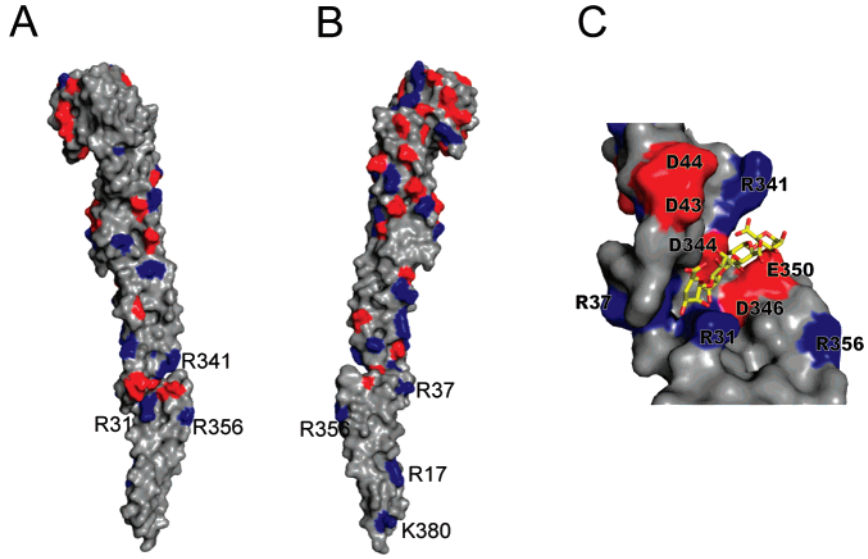

FIGURE 5: (A and B) Surface models of p5. Panel B is rotated 180° from that in panel A. Red indicates acidic residues, while blue denotes basic ones. (C) Surface of the cleft and the alginate tetrasaccharide. The tetrasaccharide coordinates were obtained from the Protein Data Bank (entry 1J1N).

(Figure 5A,B). These positively charged residues may be important in recognizing the negatively charged alginate. AlgQ1 and AlgQ2, which are periplasmic proteins in strain A1, also bind to alginate (*6*). The crystal structures of AlgQ1 and AlgQ2 complexed with alginate tetrasaccharides (PDB entries 1Y3P and 1J1N) show that these proteins bind to alginate in the cleft lined with basic and hydrophobic residues (*6*, *35*). The p5 protein also has a cleft lined with Arg near residues 20−40 and 353−363. The cleft is approximately 20 Å wide, which corresponds to the width of the alginate tetrasaccharide (Figure 5C). The cleft also contains acidic residues, i.e., Asp and Glu, and a few hydrophobic residues. The preference of a lower pH for the binding of p5 to alginate may reflect the protonation of these acidic residues. The residues forming the cleft, the so-called spoke region, are mostly conserved among flagellins. The N-terminus of this region is responsible for plant defense (*36*). The results obtained here suggest that the conserved spoke region is also involved in alginate binding, although more experiments will be necessary to prove the model in Figure 5C and details of the alginate binding properties of p5.

Role of the β-Domain. Flagellin monomers mutually interact using evolutionarily conserved N- and C-terminal regions (D0 and D1 domain). The N-terminal residues are recognized by the flagellar export system (*37*), mammalian Toll-like receptor (*38*, *39*), and plant defense receptor kinase (*36*, *40*). The C-terminal residues interact with FliS, a flagellin chaperone (*41*). We showed that alginate binds to

the N- and C-terminal regions of some bacterial flagellins. In contrast, to the best of our knowledge, there is no report that suggests the involvement of central hypervariable domains in the intermolecular interaction. The D2 and D3 domains of *Salmonella* flagellin also make relatively minor contributions to filament structure and stability (*42*, *43*).

Typical bacterial flagellins are self-assembled into external flagellar filaments for cell motility. However, different flagellin types vary in function and localization. Flagellins of spirochetes form flagella in the periplasmic space and are involved in cell motility (*44*). FlaC, a flagellin homologue of *Campylobacter jejuni*, is secreted into the extracellular milieu through the inner flagella. This secreted flagellin is believed to function as a virulence factor that binds to human epithelial cells (*45*). The central hypervariable region is missing from the secreted flagellin of *C. jejuni*. Recent reports also indicated that a mutant *Salmonella* flagellin in which most residues in the D2 and D3 domains were deleted can be transported properly to the outside of the cell but cannot form a filament (*46*). Because p5 has rather different amino acid residues in place of the amino acid residues in the D2 and D3 domains of *Salmonella* flagellin, cell-surface localization of p5 may be related to its β-domain structure.

To localize on the cell surface, p5 must be anchored to the outer membrane. Structural similarity between the p5 β-domain and the gp11 finger domain is evidence of the possibility that the β-domain interacts with other molecules because the finger domain plays an important role in associating with other proteins in the T4 phage. This possibility led us to hypothesize that the N- and C-terminal regions of strain A1 flagellin homologues are exposed to the extracellular milieu for alginate recognition through the interaction between the β-domain and cell-surface proteins.

A homology search of the β-domain (residues 170−280) of p5 using the BLAST program showed only five proteins with an *E* value higher than 10^{-4}. All of these were flagellin-homologous proteins from bacteria. Generally, it is believed that a bacteriophage is involved in horizontal gene transfer between different biomes (*47*−*49*). The finding that the finger domain of gp11 and the β-domain of p5 are similar is also of interest in the determination of the origin of these p5-like flagellin homologues.

REFERENCES

1. Hisano, T., Kimura, N., Hashimoto, W., and Murata, K. (1996) Pit structure on bacterial cell surface, *Biochem. Biophys. Res. Commun. 220*, 979−982.
2. Gacesa, P. (1988) Alginates, *Carbohydr. Polym. 8*, 161−182.
3. Wong, T. Y., Preston, L. A., and Schiller, N. L. (2000) Alginate lyase: Review of major sources and enzyme characteristics, structure-function analysis, biological roles, and applications, *Annu. Rev. Microbiol. 54*, 289−340.
4. Sawabe, T., Takahashi, H., Ezura, Y., and Gacesa, P. (2001) Cloning, sequence analysis and expression of *Pseudoalteromonas elyakovii* IAM 14594 gene (*alyPEEC*) encoding the extracellular alginate lyase, *Carbohydr. Res. 335*, 11−21.
5. Momma, K., Okamoto, M., Mishima, Y., Mori, S., Hashimoto, W., and Murata, K. (2000) A novel bacterial ATP-binding cassette transporter system that allows uptake of macromolecules, *J. Bacteriol. 182*, 3998−4004.
6. Momma, K., Mishima, Y., Hashimoto, W., Mikami, B., and Murata, K. (2005) Direct evidence for *Sphingomonas* sp. A1 periplasmic proteins as macromolecule-binding proteins associated with the ABC transporter: Molecular insights into alginate transport in the periplasm, *Biochemistry 44*, 5053−5064.
7. Hashimoto, W., Miyake, O., Momma, K., Kawai, S., and Murata, K. (2000) Molecular identification of oligoalginate lyase of *Sphingomonas* sp. strain A1 as one of the enzymes required for complete depolymerization of alginate, *J. Bacteriol. 182*, 4572−4577.
8. Yoon, H.-J., Hashimoto, W., Miyake, O., Okamoto, M., Mikami, B., and Murata, K. (2000) Overexpression in *Escherichia coli*, purification, and characterization of *Sphingomonas* sp. A1 alginate lyases, *Protein Expression Purif. 19*, 84−90.
9. Ochiai, A., Hashimoto, W., and Murata, K. (2006) A biosystem for alginate metabolism in *Agrobacterium tumefaciens* strain C58: Molecular identification of Atu3025 as an exotype family PL-15 alginate lyase, *Res. Microbiol. 157*, 642−649.
10. Aso, Y., Miyamoto, Y., Harada, K. M., Momma, K., Kawai, S., Hashimoto, W., Mikami, B., and Murata, K. (2006) Engineered membrane superchannel improves bioremediation potential of dioxin-degrading bacteria, *Nat. Biotechnol. 24*, 188−189.
11. Hashimoto, W., He, J., Wada, Y., Nankai, H., Mikami, B., and Murata, K. (2005) Proteomics-based identification of outer-membrane proteins responsible for import of macromolecules in *Sphingomonas* sp. A1: Alginate-binding flagellin on the cell surface, *Biochemistry 44*, 13783−13794.
12. He, J., Nankai, H., Hashimoto, W., and Murata, K. (2004) Molecular identification and characterization of an alginate-binding protein on the cell surface of *Sphingomonas* sp. A1, *Biochem. Biophys. Res. Commun. 322*, 712−717.
13. Underhill, C. B., and Toole, B. P. (1980) Physical characteristics of hyaluronate binding to the surface of simian virus 40-transformed 3T3 cells, *J. Biol. Chem. 255*, 4544−4549.
14. Moens, S., and Vanderleyden, J. (1996) Functions of bacterial flagella, *Crit. Rev. Microbiol. 22*, 67−100.
15. Macnab, R. M. (1996) Flagella and motility, in *Escherichia coli and Salmonella: Cellular and Molecular Biology* (Neidhardt, F. C., Curtiss, R., III, Ingraham, J. L., Lin, E. C. C., Low, K. B., Magasanik, B., Reznikoff, W. S., Riley, M., Schaechter, M., and Umbarger, H. E., Eds.) 2nd ed., Vol. 1, pp 123−145, ASM Press, Washington, DC.
16. Samatey, F. A., Imada, K., Nagashima, S., Vonderviszt, F., Kumasaka, T., Yamamoto, M., and Namba, K. (2001) Structure of the bacterial flagellar protofilament and implications for a switch for supercoiling, *Nature 410*, 331−337.
17. Yonekura, K., Maki-Yonekura, S., and Namba, K. (2003) Complete atomic model of the bacterial flagellar filament by electron cryomicroscopy, *Nature 424*, 643−650.
18. Vonderviszt, F., Kanto, S., Aizawa, S.-I., and Namba, K. (1989) Terminal regions of flagellin are disordered in solution, *J. Mol. Biol. 209*, 127−133.
19. Sanger, F., Nicklen, S., and Coulson, A. R. (1977) DNA sequencing with chain-terminating inhibitors, *Proc. Natl. Acad. Sci. U.S.A. 74*, 5463−5467.
20. Ausbel, F. M., Brent, R., Kingston, R. E., Moore, D. D., Seidman, J. G., Smith, J. A., and Struhl, K. (1987) *Current Protocols in Molecular Biology*, Wiley, New York.
21. Doublie, S., and Carter, C. W., Jr. (1992) Molecular biology for structural biology, in *Crystallization of Nucleic Acids and Proteins: A Practical Approach* (Ducruix, A., and Giege, R., Eds.) pp 311−317, Oxford University Press, New York.
22. Otwinowski, Z., and Minor, W. (1997) Processing of X-ray diffraction data collected in oscillation mode, *Methods Enzymol. 276*, 307−326.
23. Schneider, T. R., and Sheldrick, G. M. (2002) Substructure solution with SHELXD, *Acta Crystallogr. D58*, 1772−1779.
24. Sheldrick, G. M. (2002) Macromolecular phasing with SHELXE, *Z. Kristallogr. 217*, 644−650.
25. Cowtan, K., and Main, P. (1996) Phase combination and cross validation in iterated density-modification calculations, *Acta Crystallogr. D52*, 43−48.
26. Emsley, P., and Cowtan, K. (2004) Coot: Model-building tools for molecular graphics, *Acta Crystallogr. D60*, 2126−2132.
27. Murshudov, G. N., Vagin, A. A., and Dodson, E. J. (1997) Refinement of macromolecular structures by the maximum-likelihood method, *Acta Crystallogr. D53*, 240−255.
28. Laskowski, R. A., MacArthur, M. W., Moss, D. S., and Thornton, J. M. (1993) PROCHECK: A program to check the stereochemical quality of protein structures, *J. Appl. Crystallogr. 26*, 283−291.
29. DeLano, W. L. (2002) *PyMol*, DeLano Scientific, San Carlos, CA.

30. Wakabayashi, K., Hotani, H., and Asakura, S. (1969) Polymerization of *Salmonella* flagellin in the presence of high concentrations of salts, *Biochim. Biophys. Acta 175*, 195−203.
31. Leiman, P. G., Kostyuchenko, V. A., Shneider, M. M., Kurochkina, L. P., Mesyanzhinov, V. V., and Rossmann, M. G. (2000) Structure of bacteriophage T4 gene product 11, the interface between the baseplate and short tail fibers, *J. Mol. Biol. 301*, 975−985.
32. Kostyuchenko, V. A., Leiman, P. G., Chipman, P. R., Kanamaru, S., van Raaij, M. J., Arisaka, F., Mesyanzhinov, V. V., and Rossmann, M. G. (2003) Three-dimensional structure of bacteriophage T4 baseplate, *Nat. Struct. Biol. 10*, 688−693.
33. Leiman, P. G., Chipman, P. R., Kostyuchenko, V. A., Mesyanzhinov, V. V., and Rossmann, M. G. (2004) Three-dimensional rearrangement of proteins in the tail of bacteriophage T4 on infection of its host, *Cell 118*, 419−429.
34. Leiman, P. G., Shneider, M. M., Mesyanzhinov, V. V., and Rossmann, M. G. (2006) Evolution of bacteriophage tails: Structure of T4 gene product 10, *J. Mol. Biol. 358*, 912−921.
35. Mishima, Y., Momma, K., Hashimoto, W., Mikami, B., and Murata, K. (2003) Crystal structure of AlgQ2, a macromolecule (alginate)-binding protein of *Sphingomonas* sp. A1, complexed with an alginate tetrasaccharide at 1.6-Å resolution, *J. Biol. Chem. 278*, 6552−6559.
36. Felix, G., Duran, J. D., Volko, S., and Boller, T. (1999) Plants have a sensitive perception system for the most conserved domain of bacterial flagellin, *Plant J. 18*, 265−276.
37. Vegh, B. M., Gal, P., Dobo, J., Zavodszky, P., and Vonderviszt, F. (2006) Localization of the flagellum-specific secretion signal in *Salmonella* flagellin, *Biochem. Biophys. Res. Commun. 345*, 93−98.
38. Hayashi, F., Smith, K. D., Ozinsky, A., Hawn, T. R., Yi, E. C., Goodlett, D. R., Eng, J. K., Akira, S., Underhill, D. M., and Aderem, A. (2001) The innate immune response to bacterial flagellin is mediated by Toll-like receptor 5, *Nature 410*, 1099−1103.
39. Andersen-Nissen, E., Smith, K. D., Strobe, K. L., Barrett, S. L., and Cookson, B. T. (2005) Evasion of Toll-like receptor 5 by flagellated bacteria, *Proc. Natl. Acad. Sci. U.S.A. 102*, 9247−9252.
40. Zipfel, C., Robatzek, S., Navarro, L., Oakeley, E. J., Jones, J. D. G., Felix, G., and Boller, T. (2004) Bacterial disease resistance in *Arabidopsis* through flagellin perception, *Nature 428*, 764−767.
41. Evodokimov, A. G., Phan, J., Tropea, J. E., Routzahn, K. M., Peters, H. K., III, Pokross, M., and Waugh, D. (2003) Similar modes of polypeptide recognition by export chaperones in flagellar biosynthesis and type III secretion, *Nat. Struct. Biol. 10*, 789−793.
42. Yoshioka, K., Aizawa, S., and Yamaguchi, S. (1995) Flagellar filament structure and cell motility of *Salmonella typhimurium* mutants lacking part of the outer domain of flagellin, *J. Bacteriol. 177*, 1090−1093.
43. Mimori-Kiyosue, Y., Vonderviszt, F., and Namba, K. (1997) Locations of terminal segments of flagellin in the filament structure and their roles in polymerization and polymorphism, *J. Mol. Biol. 270*, 222−237.
44. Limberger, R. J. (2004) Periplasmic flagellum of spirochetes, *J. Mol. Microbiol. Biotechnol. 7*, 5493−5497.
45. Song, Y. C., Jin, S., Louie, H., Ng, D., Lau, R., Zhang, Y., Weerasekera, R., Al Rashid, S., Ward, L. A., Der, S. D., and Chan, V. L. (2004) FlaC, a protein of *Campylobacter jejuni* TGH9011 (ATCC43431) secreted through the flagellar apparatus, binds epithelial cells and influences cell invasion, *Mol. Microbiol. 53*, 541−553.
46. Malapaka, R. R. V., Adebayo, L. O., and Tripp, B. C. (2007) A deletion variant study of the functional role of the *Salmonella* flagellin hypervariable domain region in motility, *J. Mol. Biol. 365*, 1102−1116.
47. Miller, R. V. (2001) Environmental bacteriophage-host interactions: Factors contribution to natural transduction, *Antonie Van Leeuwenhoek 79*, 141−147.
48. Desplats, C., and Krisch, H. M. (2003) The diversity and evolution of the T4-type bacteriophages, *Res. Microbiol. 154*, 259−267.
49. Wommack, K. E., and Colwell, R. R. (2000) Virioplankton: Viruses in aquatic ecosystems, *Microbiol. Mol. Biol. Rev. 64*, 69−114.

BI701872X